ELSEVIER

0308-0161(95)00078-X

Int. J. Pres. Ves. & Piping **69** (1996) 97–104

0308-0161/96/$15.00

Numerical characterisation of a cylinder with circumferential cracks under pressurised thermal shock

N. K. Mukhopadhyay, B. K. Dutta, H. S. Kushwaha, S. C. Mahajan & A. Kakodkar

Reactor Design & Development Group, Bhabha Atomic Research Centre, Bombay 400085, India

(Received for publication 31 August 1995)

A numerical modelling of pressurised thermal shock (PTS) accidents has been performed. Crack growth and crack arrest are numerically simulated using the finite-element method. The analysis is done in two steps. In the first the observed crack growth phenomena has been used as input to compute parameters such as crack mouth opening displacement, *J*-integral, stress intensity factor, etc. These parameters are compared with the experimentally observed values and also with the values obtained through numerical investigations by other organisations. Crack growth and crack arrest behaviour are compared with the triaxiality parameter of the state of stress at that moment. The observed crack growth phenomena is plotted on an R–6 diagram to assess the importance of the failure assessment diagram in the evaluation of the integrity of the structure. Effort has also been directed towards studying crack growth using crack tip opening displacement criteria. In the second step, crack growth and arrest conditions have been numerically predicted using the material fracture toughness properties and compared with the experimentally observed data. Copyright © 1996 Elsevier Science Ltd.

1 INTRODUCTION

The integrity of pressurised components during a severe thermal transient is always a matter of concern to the designers. One such example is the integrity of the nuclear reactor vessel subjected to both mechanical and thermal transients. The continuing assessment of potential accident scenarios in different plants has led the US Nuclear Regulatory Commission to recognise that pressurised water reactors can experience a class of incident termed as pressurised thermal shock (PTS).[1] The thermal shock phenomena involves the possibility of the fracture of a pressurised water reactor pressure vessel subjected to emergency cooling following a loss of coolant accident (LOCA). This class of incident is characterised by the rapid cooling of the thick embrittled pressured vessel whilst at the same time primary pressure is maintained or slowly decreased during the course of the transient. Such transients have occurred in the USA and other countries[1] e.g. several years ago at the Rancho Seco Plant and others of somewhat less severity.

The significance of these transients to operating reactors is that vessel failure might result if the appropriate conditions are present at the time of the transient. The combination of the following three conditions may lead to such an incident: the presence of a flaw on the inner side of the vessel acting as a stress raiser, the low nil ductile temperature of the highly irradiated material and a severe transient cooling by injecting cold water on the inner surface of the vessel by the activation of emergency core cooling system (ECCS) during a LOCA. All these may collectively lead to propagation of the crack through the wall under the combined stress due to thermal and pressure loading.

An important aspect of the integrity evaluation is the variation of stresses and deformation

during the transient in the vicinity of a postulated flaw of limited size. Due to the cold water injection, high thermal stresses occur in the wall adjacent to the inner surface. This may also lead to high thermal stress gradients across the wall thickness. In particular, zones with existing cracks may become critical in cases of PTS loading if the nature of the stress is tensile. Due to cooling, the decrease in fracture toughness of certain materials, such as ferritic steels, may lead to a situation which is more vulnerable to failure.

The crack growth and crack arrest behaviour under thermal shock was experimentally investigated by Stumpfrock *et al.*[2] and Bass *et al.*[3] The present paper is aimed at numerically simulating the crack growth and crack arrest phenomena observed during pressurised thermal shock experiments. Several computed parameters incuding J-integral, stress intensity factor (SIF), crack mouth opening displacement (CMOD), are compared with the measured results and/or earlier published results. The crack propagation and crack arrest phenomena are also shown on a failure assessment diagram (FAD).

2 GEOMETRICAL DETAILS, MATERIAL PROPERTIES AND LOADING CONDITIONS

The details of a pressurised thermal shock experiment performed by Stumpfrock *et al.* are available in the literature.[2] A thick-walled hollow cylinder ($D_i = 400$ mm, $t = 200$ mm) was welded at both ends to the grips of a 100 MN tensile testing machine. The cylinder had a prefatigued circumferential crack of initial length 34 mm. The cylinder was made up of three materials. The precracked material was a modified 17 MoV–84 steel having a low toughness figure. This material is backed up by a hard material to arrest the crack to prevent a total failure of the thick cylinder. The various material properties are provided in Ref. 2. The cylinder was subjected to an axial pull and internal pressure. The cylinder was initially heated by an external heater. At a certain time cold water was instantaneously sprayed over the inside surface to apply severe thermal shock. The transient temperatures, crack propagation and crack mouth opening displacement (CMOD) were measured. The geometrical details are shown in Fig. 1.

3 DEVELOPMENT OF STRUCTURAL ANALYSIS CODE

The present analysis has been performed to model the observed crack growth in the above experiment by using an in-house computer code *WELTEM*[4] for nonlinear transient heat transfer analysis plus the code *THESIS*[5] for 2-D thermal elasto-plastic analysis. *WELTEM* is a finite-element code for computing transient temperatures which is capable of considering nonlinear material properties, convective or radiative boundary conditions and phase change. The modified Crank–Nicholson method and Galerkin's method are implemented for the solution of nonlinear heat transfer equations. The code *THESIS* is a thermo-mechanical finite-element code for structural analysis of plane stress, plane strain or axisymmetric problems. Thermal load can be incorporated by specifying the temperatures at each node of the structure. Material plasticity is modelled using the von Mises yield criteria, isotropic strain hardening and the Prandtl–Reuss flow rule. This code is capable of analysing temperature-dependent material properties and material creep by considering corresponding vectors of pseudo strain.

In the present analysis the J-integral is used as a measure of the intensity of crack growth. Accurate pointwise values of energy release rate $J(s)$ along a crack front are obtained using a domain integral technique. A formulation has been implemented in code *THESIS* for calculating the J-integral for 2-D thermo-mechanical cases using the domain integral expression as suggested by Shih *et al.*[6] In this formulation, a function q_1 is used which is a sufficiently smooth function in the enclosed region. The function q_1 may be assumed to vary in various patterns, such as pyramid, plateau, etc. We have defined a new type of q_1 function as a part of the present work. This new function is a combination of pyramid and plateau functions. The value of this new function q_1 is unity at the crack tip and also at the edge of the first ring surrounding the crack tip. This value is equal to zero on the edge of the domain and varies linearly between the innermost edge surrounding the crack tip and the outermost ring. It was found that this function has advantages over both the pyramid and plateau surfaces and calculations are performed using this formulation.

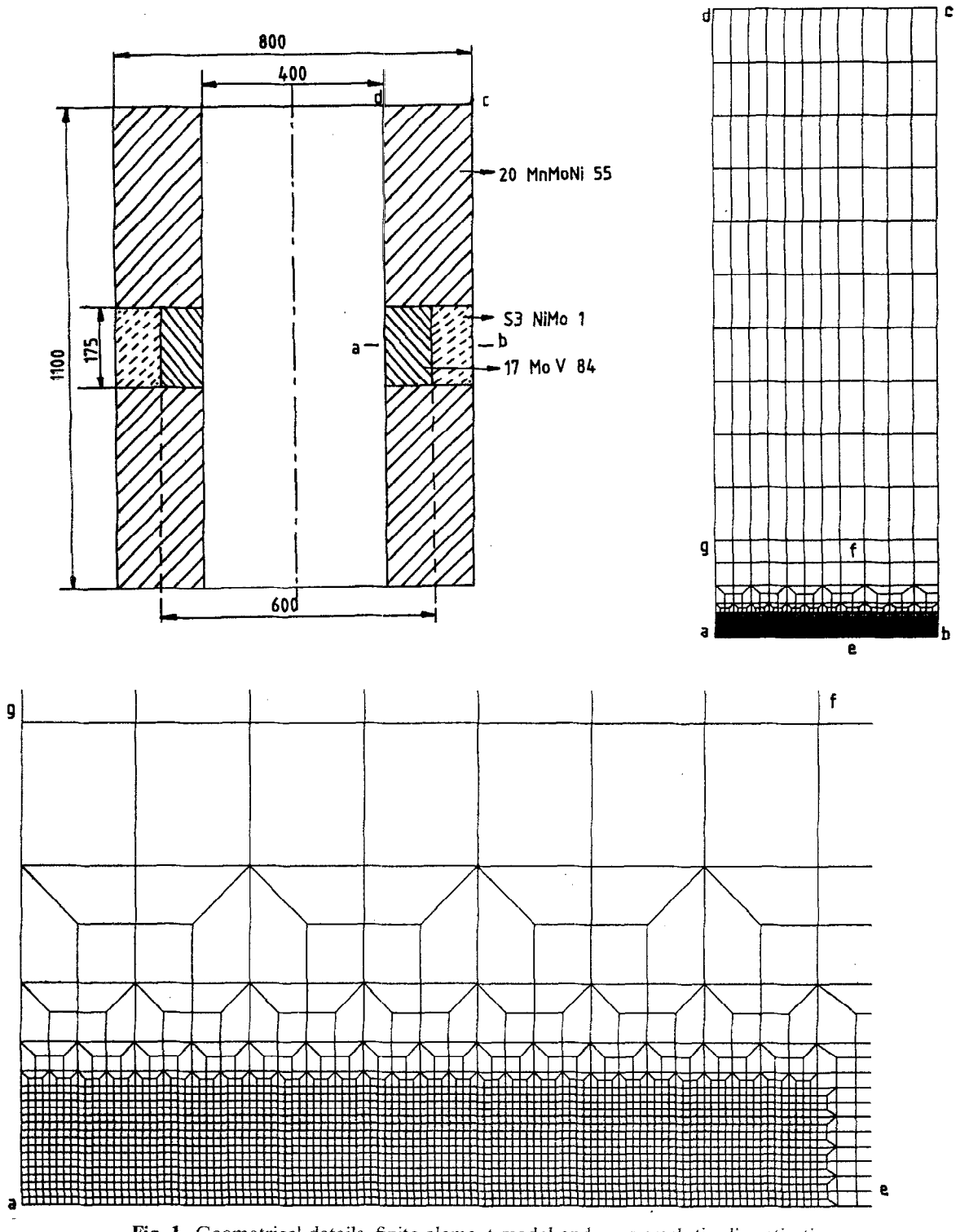

Fig. 1. Geometrical details, finite element model and near crack tip discretisation.

4 NUMERICAL INVESTIGATIONS OF PRESSURISED THERMAL SHOCK EXPERIMENT

An axi-symmetric thermo-elastic–plastic finite-element analysis was carried out including crack growth and crack arrest. The hollow cylinder was discretised employing 2627 axi-symmetric 4-node elements. The total number of nodes is 2734. The size of the element near the crack tip is made sufficiently small such that crack growth can be numerically simulated. The finite-element mesh is shown in Fig. 1. A nonlinear transient thermal analysis was performed to find out the thermal loading at various instances due to cooling using the code *WELTEM*.[4] The transient temperature

distribution along the thickness at various times is shown in Fig. 2. The thermal load was applied by specifying the earlier computed temperature at all the nodes at various time instances.

4.1 Numerical investigation based on observed crack growth

In the first part of the analysis, the crack growth and crack arrest was simulated using the observed data. A thermo-elastic–plastic analysis was carried out using the code *THESIS*.[5] The computed CMOD is plotted along with the measured CMOD[2] in Fig. 3. The variation of effective stress along the ligament at different time instants are shown in Fig. 4. The computed J-integral using a domain integral method is shown in Fig. 5. The SIF (K) is calculated from J-integral and is plotted against crack tip temperature in Fig. 6. The variation of triaxiality of stresses near the crack tip with the crack growth is shown in Fig. 7.

A number of methods are available for assessing the integrity of structures containing flaws under different loading conditions. One such method is the failure assessment diagram which is also popularly named as the R–6 method, to define a safety region for establishing the integrity of a structure with defects.[7,8] The limiting condition of a structure in the R–6 method is evaluated using fracture load and plastic collapse load. Structural integrity in

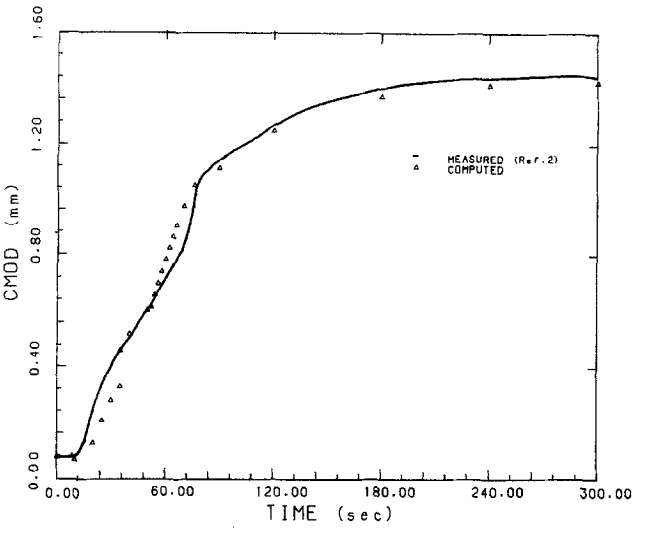

Fig. 3. Comparison of computed and measured CMOD by procedure—I.

relation to these two limiting conditions is evaluated by means of a failure assessment diagram (FAD). The procedure requires assessment points to be plotted on the FAD. The location of each assessment point depends upon the applied load, flaw size, material property, etc. A necessary criterion of acceptance of any analysis is that the assessment points of interest should lie within the area bounded by the axes of the FAD and the failure assessment line. The factor of safety associated with the point is the ratio of the distance of a point on FAD from origin lying on the same straight line

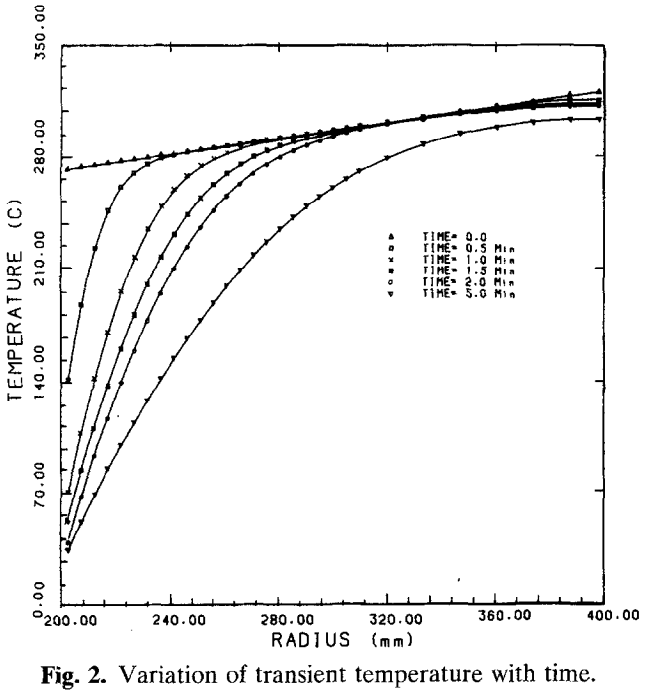

Fig. 2. Variation of transient temperature with time.

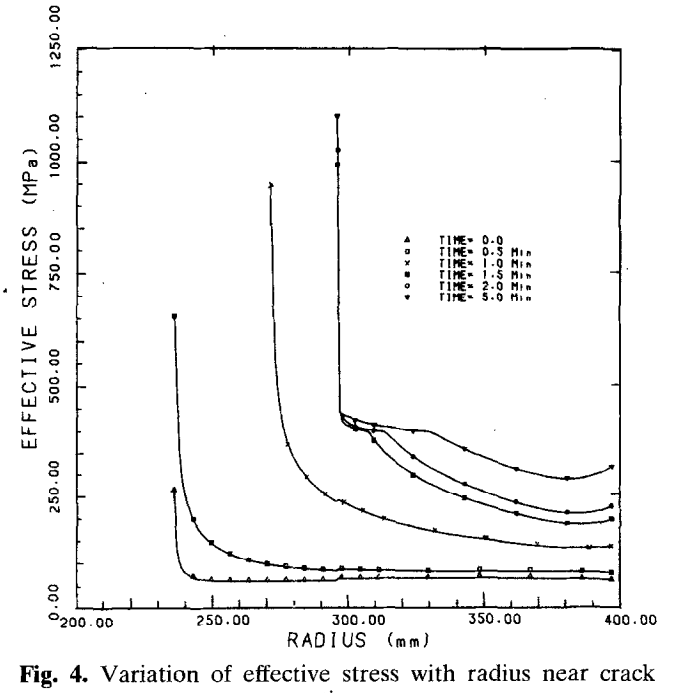

Fig. 4. Variation of effective stress with radius near crack tip.

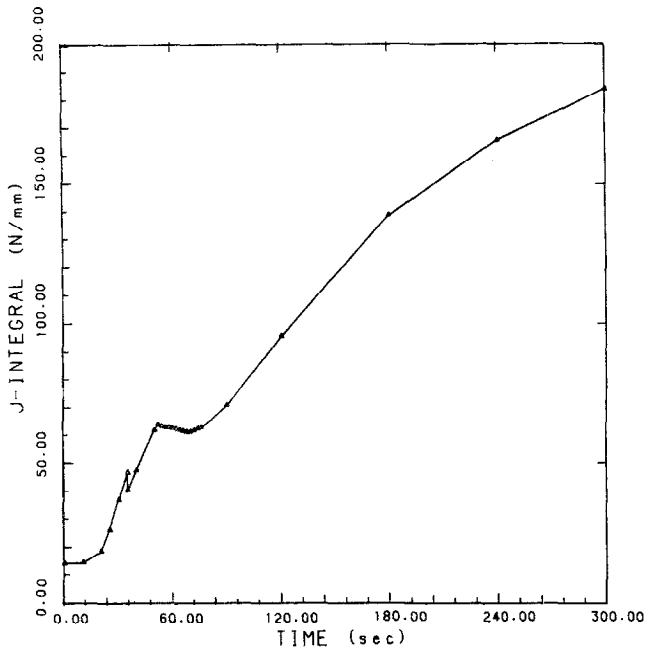

Fig. 5. Variation of J-integral with time.

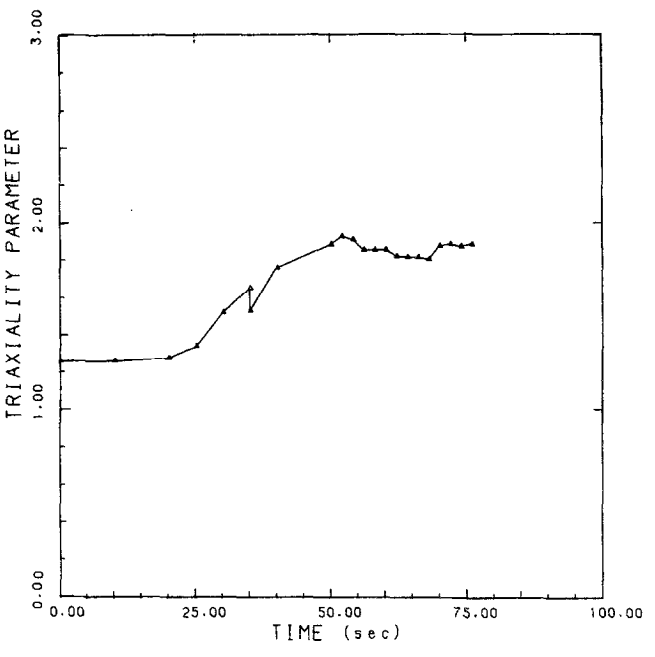

Fig. 7. Variation of triaxiality parameter near crack tip with time.

as the assessment point and the distance of the assessment point from the origin.

The crack growth and crack arrest phenomena is plotted on an FAD which can be drawn using either Option I or Option II.[8] The Option I FAD is described by the following equation:

$$\mathrm{Kr} = (1 - 0{\cdot}14\mathrm{Lr}^2)[0{\cdot}3 + 0{\cdot}7\exp(-0{\cdot}65\mathrm{Lr}^6)] \quad \text{for} \quad \mathrm{Lr} \leq \mathrm{Lr}^{\max}$$
$$\mathrm{Kr} = 0 \quad \text{for} \quad \mathrm{Lr} \geq \mathrm{Lr}^{\max} \qquad (1)$$

In order to derive this diagram only the engineering values of the lower yield or 0·2% proof stress and the flow stress need to be known. In certain circumstances where the initial rate of hardening of the stress/strain curve is high, this option underestimates the flaw tolerance of the structure. The Option II FAD is drawn using the following relationship:

$$\mathrm{Kr} = \left[\frac{\mathrm{E}\varepsilon_{\mathrm{ref}}}{\mathrm{Lr}\sigma_{\mathrm{Y}}} + \frac{\mathrm{Lr}^3\sigma_{\mathrm{Y}}}{2\mathrm{E}\varepsilon_{\mathrm{ref}}}\right]^{-0{\cdot}5} \qquad (2)$$

Here E denotes elastic modulus, σ_{Y} is the yield stress and $\varepsilon_{\mathrm{ref}}$ is the reference strain. The collapse load is calculated on the basis of the collapse of the remaining ligament which is assumed to occur when the induced stress exceeds the flow stress. The thermal load is converged into equivalent primary load and summed with initial primary load to compute the total applied load on the structure. The condition of crack tip on the R–6 diagram is demonstrated in Fig. 8. The abrupt change in the state of the crack tip on this diagram is due to crack propagation. The two types of crack propagation during the present experiments are shown in this diagram. These are cleavage fracture between a–b and stable crack growth between c–d as shown in Fig. 8. The factor of safety with time from this diagram as suggested in Ref. 8 is shown in Fig. 9.

The crack tip opening displacement (CTOD) is another parameter which can be used to characterise crack growth. This parameter is correlated with J or K as shown in the following relationship:

$$\delta = \frac{J}{\sigma_{\mathrm{Y}}} = \frac{K^2(1-\nu^2)}{\sigma_{\mathrm{Y}}\mathrm{E}}. \qquad (3)$$

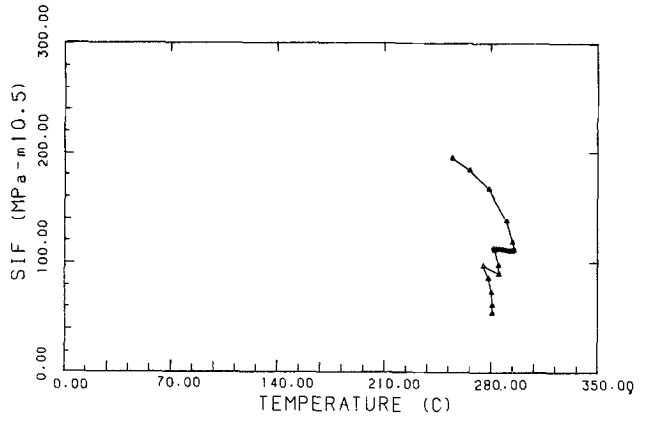

Fig. 6. Variation of stress intensity factor with crack tip temperature.

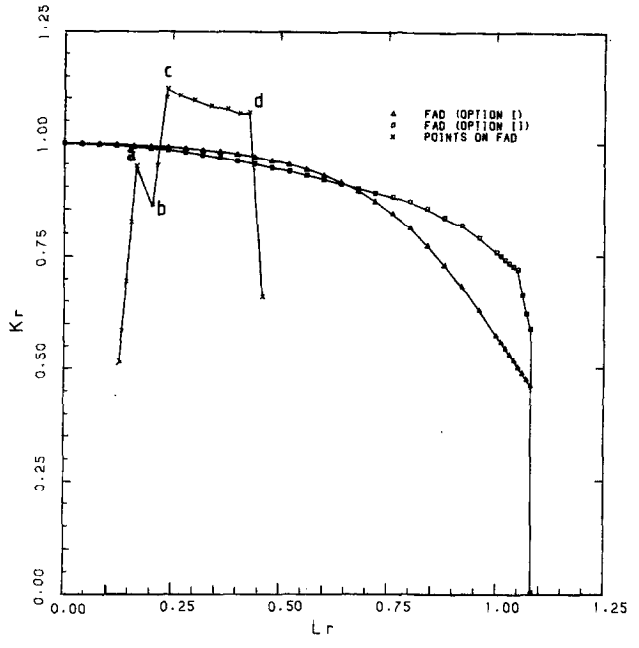

Fig. 8. The path of assessment points during crack propagation on FAD.

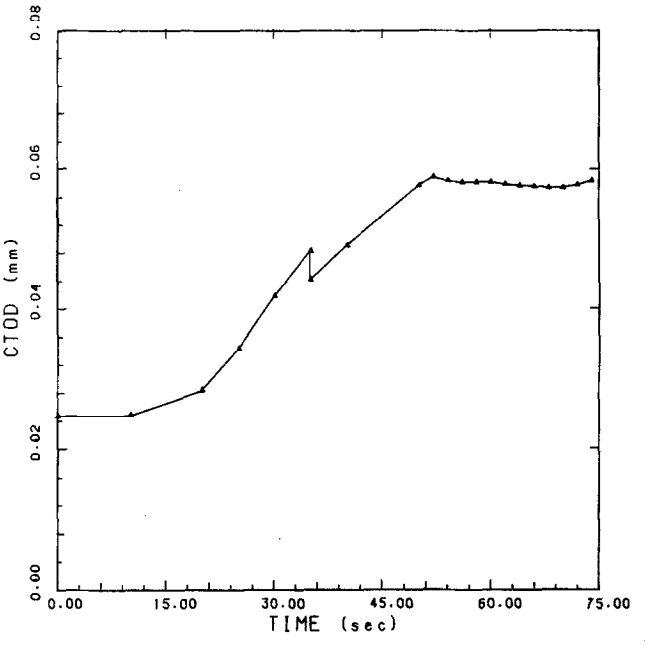

Fig. 10. Variation of crack tip opening displacement with time during crack growth.

Here ν denotes Poisson ratio. It is postulated that fracture occurs at a critical value of CTOD defined as δ_c. This δ_c can be determined from experiment; however it can also be determined indirectly by using eqn (3). It is observed that the crack tip temperature during the crack growth varies from 274°C to 294°C. The value of δ_c as calculated using material fracture toughness data in that temperature range is found to be 0·054 to 0·058 mm. In the following analysis using a finite-element method, the CTOD is computed. This variation of CTOD with time is shown in Fig. 10.

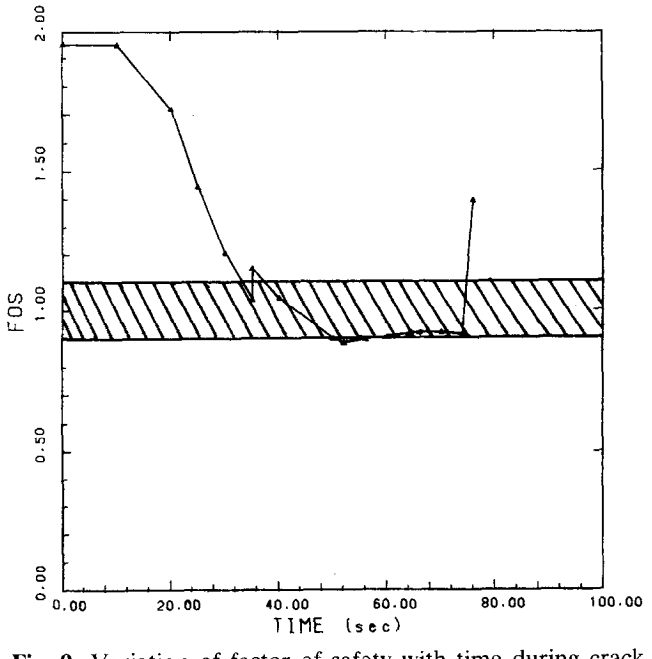

Fig. 9. Variation of factor of safety with time during crack propagation based on FAD.

4.2 Numerical investigation by predicting crack growth using material properties

In the second part of this investigation the crack extension is predicted by using material fracture toughness data. The fracture toughness data[2] shows a large scatter of both K_{Ic} and K_{Ia} with temperature. The average K_{Ic} value is used in the subsequent analysis. The K_{Ia} during the cleavage event has been considered to be 11% less than the K_{Ic} value at that temperature. Using these values the cleavage event is simulated. It is observed that the cleavage event starts at 37 s. and total extension of crack length is by 20 mm. The analysis is continued to cover the stable growth of the crack. The computed crack mouth opening displacement (CMOD) is shown in Fig. 11.

5 DISCUSSION

The computed temperature transients along the wall thickness have excellent agreement with the measured temperature values as presented in Ref. 2. These temperature values represent the

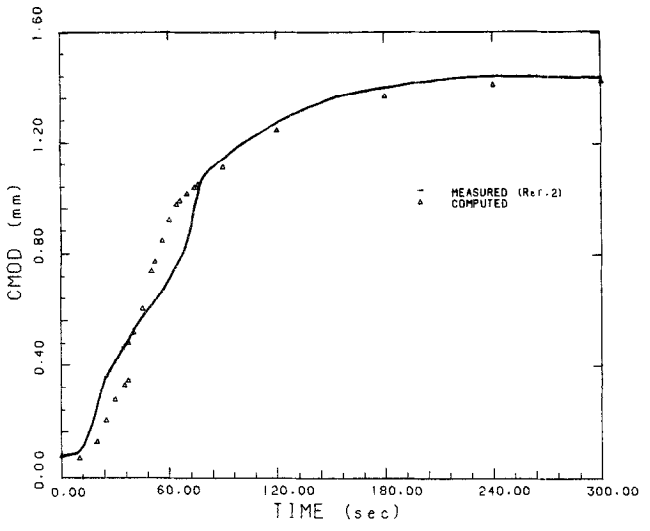

Fig. 11. Comparison of computed and measured CMOD by procedure—II.

intensity of thermal shock over the wall thickness at different time instants. The computed CMOD has good agreement with measured values as shown in Fig. 3. The effective stresses along the remaining ligament indicating the plastic zone are shown in Fig. 4. This figure also shows the extension of the plastic zone near the crack tip with time. The thermal load and the SIF increase and the crack tip temperature decreases with time for a stationary crack during the cooling. The variation of SIF with crack tip temperature is shown in Fig. 6. During the cleavage event there is a sharp drop in SIF value due to a decrease in thermal load. The crack tip temperature during this event increases as the crack tip moves to a higher temperature zone. After this event, the SIF steadily increases and the crack tip temperature decreases as the crack remains stationary. During the stable crack growth phenomena, the SIF is nearly constant and drops by only a marginal value. The constant SIF indicates that the increase in crack extension is neutralised by the reduction in thermal load in the expression of SIF.

The degree of triaxiality of the stresses in the vicinity of the crack tip may quantitatively be expressed by the triaxiality parameter h defined as:

$$h = \frac{\sigma_m}{\sigma_v} \tag{4}$$

where σ_m is the hydrostatic stress and σ_v is the von Mises equivalent stress. The effect of stress triaxiality parameter h on crack initiation using a damage model concept has been presented in the literature.[9,10] Spontaneous fracture of the specimen or components without previous stable crack extension is expected if the triaxiality parameter h attains or is above a critical value h_c in front of the crack tip. A critical value of the h_c value is quoted as 1·925 in Ref. 2. The other necessary criteria is that the effective crack initiation value J_{Ic} must be reached or exceeded to initiate crack propagation. Figure 7 shows that triaxiality parameter h has values between 1·9 to 2·0 throughout the stable crack growth period. However, this value is approximately 1·65 at the instance of cleavage fracture.

The crack propagation and the crack growth phenomena as observed during the experiment have been plotted on the FAD. Figure 8 shows that the cleavage occurs before the assessment point could reach the failure assessment line. After the cleavage, K drops due to crack propagation. The crack gets arrested once the factor of safety has improved. Steady-state crack propagation is not found to initiate immediately after the point reaches the assessment line. It is rather found to start beyond the boundary of FAD. During the entire stable crack propagation period the assessment points are outside the area of FAD. After the stable propagation is over the assessment point is again within the FAD concluding the arrest of the crack at the outer tough material. It is observed from Fig. 9, that crack growth phenomena occurs within a value of factor of safety $=1{\cdot}0 \pm 0{\cdot}1$. This zone may be treated as an uncertain zone for the present experiment in the R–6 approach and crack propagation is expected from any point in this zone.

6 CONCLUSIONS

The following conclusions are drawn from the above analysis:

(1) The newly developed q_1 function, which is a combination of pyramid and plateau functions, is found to compute the J-integral with good agreement.

(2) The good agreement of the computed CMOD with that of the measured CMOD shows that numerically crack growth can be simulated using gradual release of nodes.

(3) The crack growth and arrest phenomena is

plotted on the R–6 plane using average material fracture toughness data. A zone of uncertainty is found to exist for the present crack growth phenomena near the assessment line. It is observed that the propagation events are confined (start and arrest) to this uncertainty zone with the factor of safety between $1 \pm 0{\cdot}1$.

(4) An attempt has been made to use the concept of triaxiality state of stress to explain the crack growth and arrest phenomena. The analysis shows that the computed triaxiality parameter h has a value between 1·9 and 2·0 throughout the stable crack propagation period. However, this value is approximately 1·65 at the instant of cleavage fracture. No firm conclusion could be drawn about the role of the triaxiality parameter in explaining stable/unstable crack propagation in the present problem.

(5) The computed CTOD using the finite-element method has a nearly constant value of 0·058 mm during the stable crack growth period. This value also has good agreement with the δ_c calculated from material fracture toughness data in that temperature range. However, the CTOD computed at the onset of cleavage is found to be lower than δ_c. Hence, the stable crack growth can be simulated using CTOD criterion in the present case.

(6) The second analysis procedure shows that the crack growth can be simulated using an average value of K_{Ic}. The computed CMOD is found to match well with the measured value.

REFERENCES

1. Serpan, C. Z. Jr., USNRC materials research for evaluation of pressurised thermal shock in RPV of PWRs, *Nucl. Engng Design*, **80** (1980) 53–63.
2. Stumpfrock, L., Ross, E., Huber, H. & Weber, U., Fracture mechanics investigations on cylindrical large-scale specimens under thermal shock loading, *Nucl. Engng Design*, **144** (1993) 31–44.
3. Bass, B. R., Pugh, C. E., Keeney-Walker, J., Schulz, H. & Sievers, J., Assessment of ductile fracture methodology based on applications to large-scale experiments, *Structural Mechanics In Reactor Technology*, **11** (G02/1) (Aug. 1991) 25–36.
4. Dutta, B. K., Kushwaha, H. S. & Kakodkar, A., Computer programme *WELTEM* (analysis of two-dimensional heat transfer problems by finite-element technique): Theory and user's manual, B.A.R.C./I-671, Bombay, 1981.
5. Dutta, B. K., A 2-D thermo-mechanical finite-element model for residual stress determination during welding and annealing, M. Tech Thesis, Mechanical Engng Dept., I.I.T. Kanpur, July 1983.
6. Shih, C. F., Moran, B. & Nakamura, T., Energy release rate along a three-dimensional crack front in a thermally stressed body, *Int. J. Fract.*, **30** (1986) 79–102.
7. Chell, G. G., A procedure for incorporating thermal and residual stresses into the concept of a fracture assessment diagram, in *Elastic-Plastic Fracture* (eds. Landes J. D., Begley J. A. & Clarke G. A.), ASTM, STP 668, 581, 1979.
8. Milne, I., Ainsworth, R. A., Dowling, A. R. & Stewart, A. T., Assessment of the integrity of structures containing defects, *Int. J. Pres. Ves & Piping*, **32** (1988) 3–104
9. Zheng, M., Luo, Z. J. & Zheng, X., A new damage model for ductile materials, *Engng Fract. Mech.*, **41** (1992) 103–110.
10. Zheng, M., Hu, C., Luo, Z. J. & Zheng, X., Further study of the new damage model by negative stress triaxiality, *Int. J. Fract.*, **63** (1993) R15–R19.